Petroleum Science (2019) 16:252–266
https://doi.org/10.1007/s12182-018-0293-3

ORIGINAL PAPER

Geochemistry of upper Permian siliceous rocks from the Lower Yangtze region, southeastern China: implications for the origin of chert and Permian ocean chemistry

Zhi-Wei Liao[1,2,3,4] · Wen-Xuan Hu[5] · Xiu-Gen Fu[3] · Zhong-Ya Hu[5]

Received: 27 June 2018 / Published online: 29 December 2018

Abstract

The Permian Chert Event is of great significance to understanding the geological evolution of the entire Permian; however, the origin of widespread chert formation is debated. We report new geochemical data from deep-marine siliceous rocks of the upper Permian Da-long Formation, Lower Yangtze region, southeastern China. Their geochemical results show that these thin-bedded siliceous rocks have a clear biologic origin, with rare to no evidence of hydrothermal influence. The values of Al/(Al + Fe + Mn) and Eu/Eu* are 0.60–0.84 (mean = 0.72) and 0.45–1.08 (mean = 0.77), respectively, and Mn/Ti ratios are relatively low (mean = 0.72). The correlations of La_N/Ce_N, La_N/Yb_N, and Fe_2O_3/TiO_2 with $Al_2O_3/(Al_2O_3 + Fe_2O_3)$, along with the Ce anomaly, indicate that the Da-long siliceous rocks were deposited at a transitional zone between a continental margin and the open ocean; i.e., relatively close to terrestrial sediment input and far from hydrothermal activity. The accumulation of chert is related to its unique paleogeographic location in an equatorial setting with many submarine paleo-highlands. Intense upwelling and frequent local volcanism are the main factors that promoted the development of siliceous rocks in the studied area. Ocean acidification triggered by large-scale volcanism (Large Igneous Province) during the late Permian led to extensive silica precipitation and preservation.

Keywords Lower Yangtze region · Da-long Formation · Siliceous rock · Biological chert · Volcanism

Edited by Jie Hao

✉ Zhi-Wei Liao
zwliao16@cqu.edu.cn

✉ Wen-Xuan Hu
huwx@nju.edu.cn

[1] State Key Laboratory of Coal Mine Disaster Dynamics and Control, College of Resources and Environmental Science, Chongqing University, Chongqing 400044, China

[2] Shandong Provincial Key Laboratory of Depositional Mineralization and Sedimentary Mineral, Shandong University of Science and Technology, Qingdao 266590, Shandong, China

[3] Key Laboratory of Sedimentary Basin and Oil and Gas Resources, Ministry of Land and Resources, Chengdu 610081, China

[4] State Key Laboratory of Palaeobiology and Stratigraphy (Nanjing Institute of Geology and Palaeontology, CAS), Nanjing 210008, Jiangsu, China

[5] State Key Laboratory for Mineral Deposits Research, School of Earth Sciences and Engineering, Institute of Energy Sciences, Nanjing University, Nanjing 210023, Jiangsu, China

1 Introduction

Siliceous rock or chert is a common sedimentary rock that consists mainly of microcrystalline or cryptocrystalline quartz (Bates and Jackson 1980). These rocks are widespread in a range of sedimentary environments including continental margins, island arcs, and ocean ridges (Jones and Murchey 1986). Various periods in the Earth's history have seen significant chert accumulation (Maliva et al. 1989), such as the Permian (Murchey and Jones 1992), late Triassic (Ritterbush et al. 2015), and Eocene (McGowran 1989). Thus, the origin of siliceous rocks is important in understanding the evolutionary history, paleogeography, paleoceanography, and paleotectonic setting of ancient marine environments (Shimizu and Masuda 1977; Aitchison and Flood 1990; Murray et al. 1990, 1991; Murchey and Jones 1992; Murray 1994; Kato et al. 2002; Yao et al. 2013; Lv and Chen 2014; Ritterbush et al. 2015; Han et al. 2015; Hu et al. 2017; Lv et al. 2017; Pang et al. 2018).

South China is part of the Tethyan archipelagic ocean system (Yin et al. 1999), where multilayer siliceous sediments

were deposited during the Permian, including the Gufeng Formation (Kametaka et al. 2005), the Maokou Formation (Qiu and Wang 2011), the Wujiaping Formation (Tian et al. 2007), and the Da-long Formation (e.g., Feng and Algeo 2014). In particular, the genesis of thin-bedded cherts of the Da-long Formation is of great interest as they may relate to the cause of largest mass extinction in the Earth's history, i.e., the Latest Permian Extinction (e.g., Shen et al. 2012). Moreover, the Da-long siliceous rocks are organic-rich and brittle and thus are considered to have potential for hydrocarbon generation within this region (Cao et al. 2015).

It is debated whether the Da-long Formation cherts are biogenic or hydrothermal in origin (Yao et al. 2013; Cheng et al. 2015). For example, thin-bedded cherts of the Da-long Formation in southeastern Hubei Province and southern Anhui Province in the Middle Yangtze region are considered to be hydrothermal in origin (Xu 1997; Zeng et al. 2004), whereas cherts in the Zhaojiaba section, from a similar region, are thought to be biogenic (Yu et al. 2012). Some cherts containing siliceous organisms from the Middle-Upper Yangtze region are combined biogenic and hydrothermal in origin, e.g., Zhaoguya (Lei et al. 2002), Luodian (Li et al. 2009), and Shangsi (Chen et al. 2012). This suggests that the genesis of the Da-long cherts is very complex and controlled by many factors. In fact, multiple origins have been proposed for the Da-long cherts (Lei et al. 2002; Li et al. 2009; Chen et al. 2012). Numerous studies have examined the Da-long Formation in the Middle and Upper Yangtze region (Xu 1997; Tian et al. 2007; Chen et al. 2012; Yu et al. 2012; Shi et al. 2015, 2018). However, only few samples from a limited number of sections from the Lower Yangtze region have been studied (Cheng et al. 2015). In addition, previous studies mainly used conventional petrological and sedimentological observations to investigate the genesis of the Da-long cherts, and the absence of any systematic geochemical analysis has limited our understanding of the environment in which the cherts of the Da-long Formation originated and their processes of formation. However, geochemical constraints are critical to understand these issues, especially the hydrothermal origin of the cherts (Chen et al. 2012).

Here, we report the detailed geology and geochemistry of siliceous rocks from three well-preserved Da-long Formation deep-water sections that have recently been discovered in the Lower Yangtze region, and discuss the genesis of the Da-long cherts and ocean chemical conditions during the late Permian.

2 Geological setting

The Lower Yangtze region is located within the Yangtze Platform, at the northeastern margin of the Yangtze Block in South China (Fig. 1a). The region has a NE–SW structural trend (Fig. 1b), and at the time of the Permian–Triassic Boundary (PTB), it was connected to the Qinling paleo-ocean to the northwest and to the Cathaysian Block to the southeast (Yin et al. 1999). The region was located in a shallow-water delta plain setting during the Wuchiapingian stage, in a deep-water basin setting during the early Changhsingian stage at a time of sea-level transgression, and in a relatively deep-water setting in the Early Triassic Yinkeng interval during a sea-level regression (Anhui Provincial Geological Bureau 1987; Du et al. 2010).

The Niushan, Changqiao, and Caicun sections are located in a sedimentary depression in the Lower Yangtze

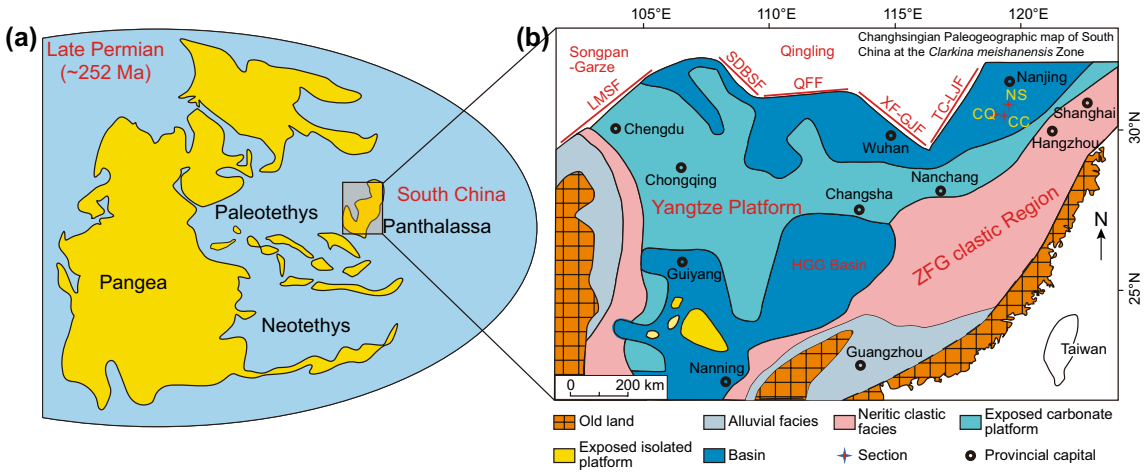

Fig. 1 **a** Global paleogeographic map for the Permian–Triassic Boundary interval (ca. 252 Ma) (modified after Shen et al. 2012), **b** simplified paleogeography of the South China block during the late Permian and the location of the studied sections (modified after Feng and Gu 2002). Red stars mark the locations of the Niushan (NS), Changqiao (CQ), and Caicun (CC) sections

region at Xuancheng City, southern Anhui Province. Quarrying activity at these three sections has exposed fresh chert that is ideal to study. Stratigraphically, the outcrops in the study area comprise the upper Permian Longtan and Da-long Formations, and the Lower Triassic Yinkeng Formation. The sedimentology and petrology of the Da-long Formation indicate that it records a complete sea-level cycle from transgression to regression (Fig. 2; Liao et al. 2016a). The Da-long Formation is dominated by black fine-grained rocks, including black mudstone, chert, siliceous mudstone, calcareous mudstone, and carbonate. The formation can be divided into three units based on sedimentary and lithological features. The sections investigated in this study are distributed mainly in the middle of the three Da-long Formation sections (Fig. 2).

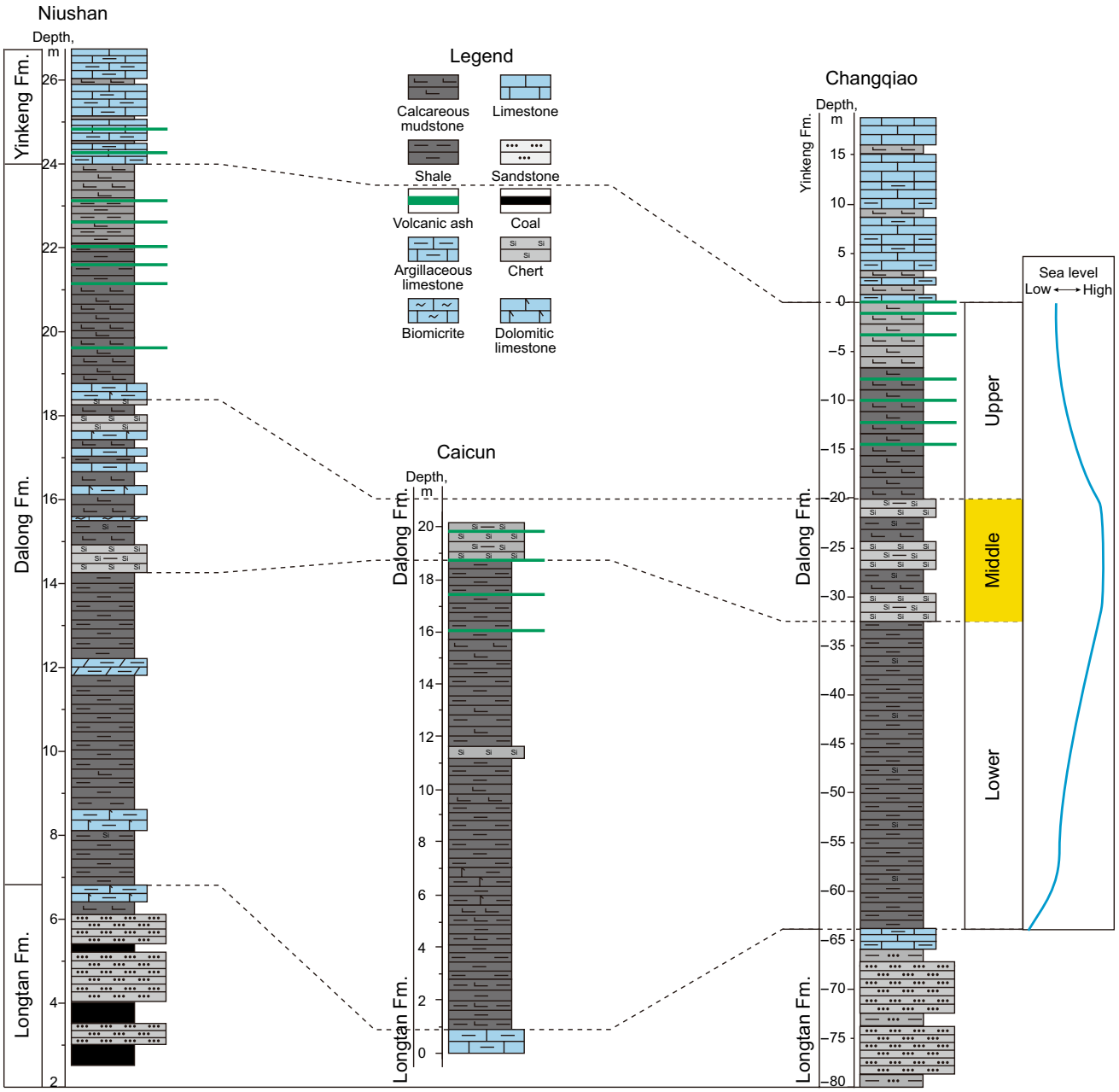

Fig. 2 Stratigraphic correlation of Da-long Formation in the southern Anhui Province, China. Note that the yellow area represents the siliceous rock layers

3 Methods

A total of 47 siliceous rock samples were collected from the three studied sections (Fig. 1b). Whole-rock samples were crushed in a corundum jaw crusher to 60 mesh. Approximately 60 g of each sample was powdered in an agate ring mill to 200 mesh.

Whole-rock major-element and trace-element geochemical analyses were carried out at the State Key Laboratory for Mineral Deposits Research, Nanjing University, China. An X-ray fluorescence (XRF) spectrometer (ARL9800XP) was used for major-element analyses, and a Finnigan Element II ICP–MS was used for trace-element analyses. The analytical precision of major-element analyses was better than 2% for all elements. The analytical procedures used for trace elements followed those of Gao et al. (2003). Calibration against USGS rock standards (BHVO–2, AGV–2, BCR–2, and GSP–1) indicates a precision and accuracy better than 5% for Sc, V, Co, Zn, Rb, Sr, Y, Nb, Cs, Ba, Th, and rare earth elements (REEs), and 10% for Li, Cu, Zr, Hf, Ta, Pb, and U.

In this study, Ce and Eu anomalies were calculated following Zhao and Gao (1998), as follows: $Ce/Ce^* = Ce_N/(La_N \times Pr_N)^{1/2}$ and $Eu/Eu^* = Eu_N/(Sm_N \times Gd_N)^{1/2}$. Titanium (Ti) was used to calculate the abundance of non-detrital or excess elements (e.g., Al_{xs}, Mn_{xs}, Fe_{xs}), thus excluding the terrigenous contribution of these elements (Chen et al. 2012). The non-detrital contribution was calculated as follows:

$$Element_{xs} = Element_{total} - Ti_{total} \times (Element/Ti)_{NASC}.$$

4 Results

The siliceous rocks of the Da-long Formation are black, thin-bedded, extremely hard and show well-developed joints, horizontal bedding, and rare or no bioturbation (Fig. 3a–c). The thickness of siliceous rocks in the three section ranges from approximately 2 (Caicun) to 10 m (Changqiao), and the proportion of the siliceous layers in the Da-long Formation is relatively low (< 15%) (Fig. 2). Some sections contain abundant lamellar pyrite nodules (Fig. 3c) and beds of pale green volcanic ash (Fig. 3b). The siliceous rocks contain abundant radiolarians and sponge spicules, but no benthos (Fig. 4a–k). Most of the sponge spicules are > 200 μm long (Fig. 4e–f). The radiolarian fossils are rounded to subrounded and 50–100 μm wide (Fig. 4h–k). Framboidal pyrite is common in most samples (Fig. 4l).

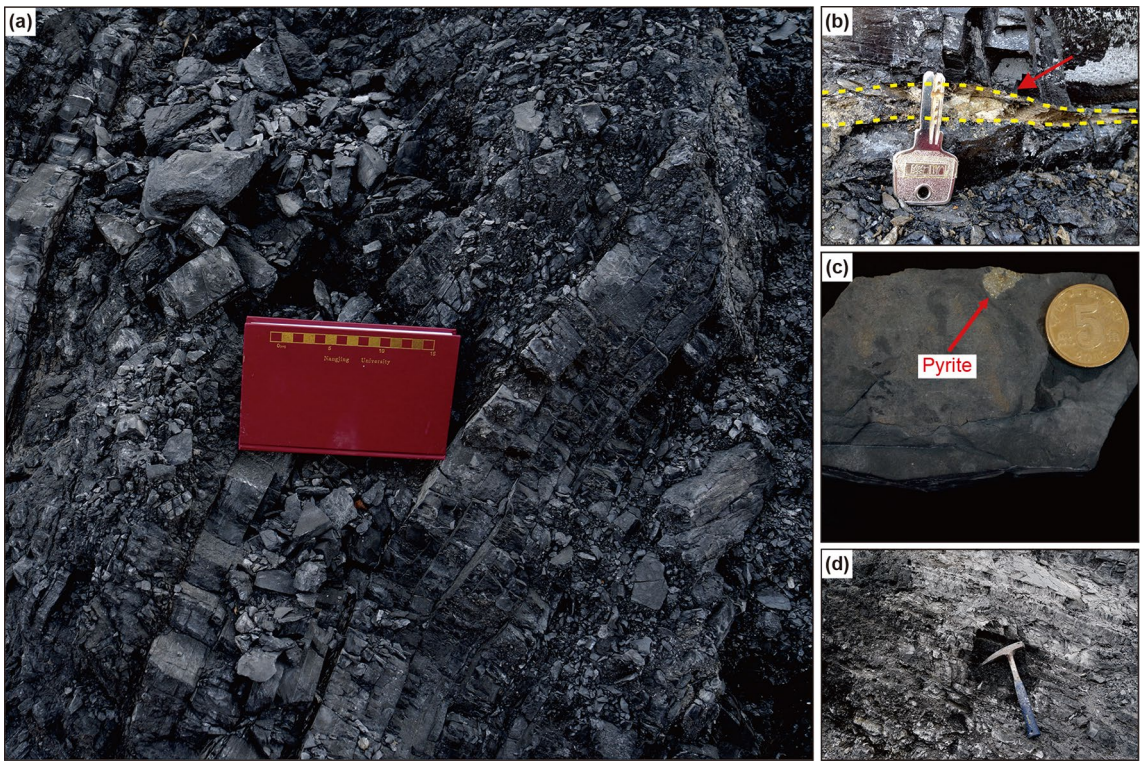

Fig. 3 Outcrop photographs of the upper Permian Da-long Formation in southern Anhui Province. **a** Thin-bedded siliceous rocks in the Changqiao section, **b** volcanic ash layer (arrowed) of the Da-long Formation in the Caicun section, **c** lamellar pyrite nodules in the Niushan section, **d** thin-bedded siliceous rocks in the Niushan section

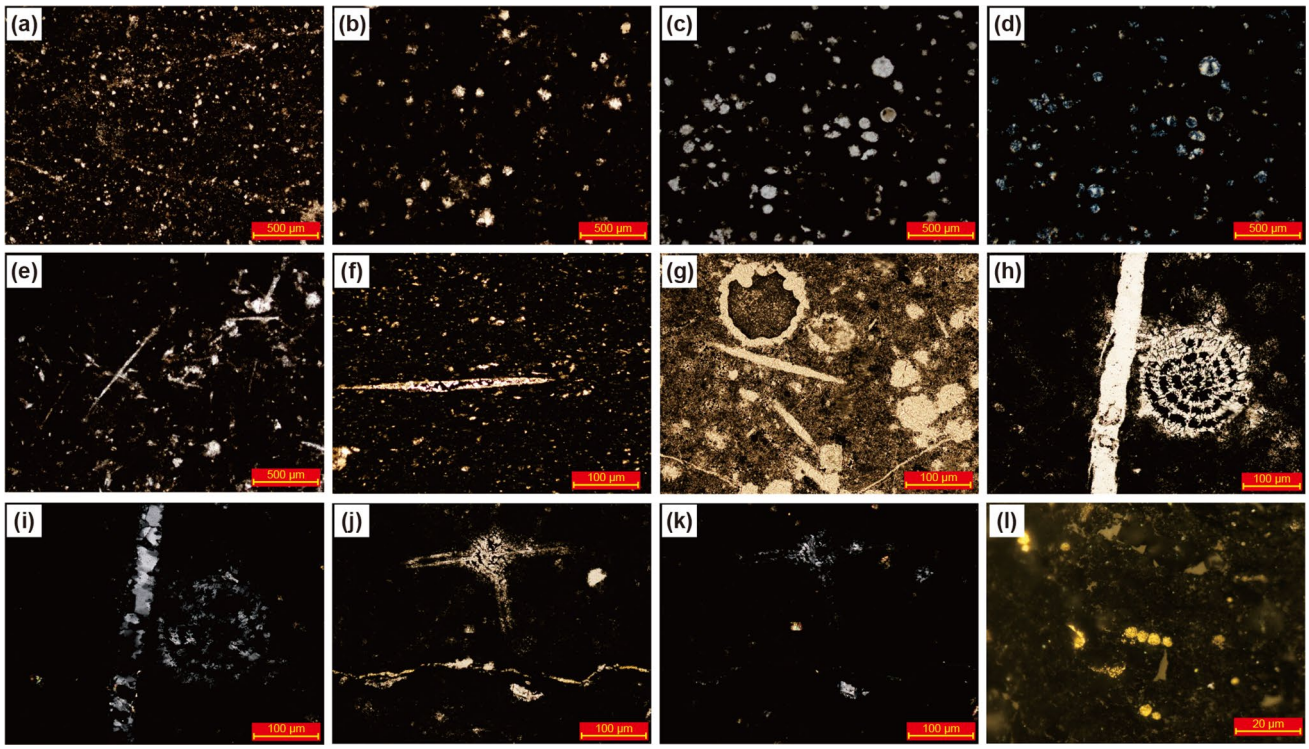

Fig. 4 Typical thin-section features of the Da-long Formation cherts. **a** Organic-rich chert containing bioclastics, Caicun section (plane-polarized light), **b** black chert containing irregular siliceous grains, Caicun section (plane-polarized light), **c** thin-bedded chert containing round radiolarian tests, Changqiao section (plane-polarized light), **d** as in **c**, but cross-polarized light, **e** siliceous rock with sponge spicules, Changqiao section (plane-polarized light), **f** siliceous rock with sponge spicules, Niushan section (plane-polarized light), **g** chert containing siliceous biodetritus, Niushan section (plane-polarized light), **h** chamber structure of a radiolarian test, Niushan section (plane-polarized light), **i** as in **h**, but cross-polarized light, **j** siliceous rock containing sponge spicules, Niushan section (plane-polarized light), **k** as in **j**, but cross-polarized light, **l** chert containing framboidal pyrite, Niushan section (plane-polarized light)

The geochemical data show that the SiO_2 content of siliceous rocks ranges from 60.1 to 91.6 wt% with a mean of 76.3 wt% (Table 1). All samples contain MnO, ranging from 0.0005 to 0.04 wt% (mean = 0.015 wt%). The Al_2O_3 content ranges from 1.60 to 10.4 wt% (mean = 5.42 wt%). The Al/(Al + Fe + Mn) ratio varies from 0.60 to 0.85 (mean = 0.73), the Si/(Si + Fe + Al) ratio varies from 0.80 to 0.97 (mean = 0.90), and the Mn/Ti ratio varies from 0.005 to 0.64 (mean = 0.14).

The content of total earth rare elements ($\sum$REE) ranges from 20 to 240 ppm (mean = 120 ppm), the Ce anomaly varies from 0.62 to 1.86 (mean = 1.06), the Eu anomaly varies from 0.45 to 1.08 (mean = 0.77), the La_N/Ce_N ratio ranges from 0.58 to 2.55 (mean = 1.18), the La_N/Yb_N ratio varies from 0.36 to 4.69 (mean = 1.45), and the Y/Ho ratio varies from 11.3 to 68.6 (mean = 34.9).

5 Discussion

5.1 Origin of siliceous rocks

The origin of silica, the depositional environment, and formation mechanisms are three fundamental areas of interest in siliceous rock research (e.g., Murchey and Jones 1992; Murray 1994; Kametaka et al. 2005). Biological or biochemical precipitation (e.g., Kametaka et al. 2005), hydrothermal activity (e.g., Chen et al. 2006), and their combined actions (e.g., Chen et al. 2012) are regarded as the most common sources of siliceous rocks. Previous studies on extensive chert accumulations have examined Precambrian marine hydrothermal systems (e.g., Fan et al. 2013;

Table 1 Geochemical data of siliceous rocks from the Da-long Formation, Lower Yangtze region, Southeast China

Samples	SiO_2, wt%	Al_2O_3, wt%	Total REE, ppm	Y/Ho	Al/(Al + Fe + Mn)	Si/(Si + Fe + Al)	Mn/Ti	La_N/Yb_N	La_N/Ce_N	Ce/Ce*	Eu/Eu*
CC-26	86.6	5.45	93	31	0.79	0.92	0.04	0.91	0.73	1.6	1.37
CC-25	80.1	5.73	229	28	0.74	0.9	0.06	1.41	0.72	1.47	0.81
CC-24	77.5	5.32	240	11.3	0.67	0.9	0.06	0.74	1.26	0.82	0.69
CC-22	63	9.4	194	27.7	0.72	0.81	0.09	1.95	1.33	0.83	0.97
CC-21	62.5	9.28	210	26.3	0.71	0.81	0.08	1.96	1.33	0.82	0.93
CC-20	60.1	8.85	215	27.7	0.68	0.8	0.09	2.11	1.32	0.82	1.01
CC-18	64.3	4.67	163	29.3	0.73	0.9	0.19	1.93	0.62	1.78	1
CC-16	63	9.06	236	28.5	0.76	0.83	0.09	1.98	0.64	1.74	0.99
CC-15	66	8.9	240	27.2	0.76	0.83	0.07	2.41	0.58	1.86	0.94
CC-11	82.4	3.34	102	28.9	0.8	0.95	0.09	1.85	0.7	1.51	0.9
CC-10	65.5	1.6	101	31.8	0.78	0.97	0.32	2.5	1.01	1.11	1.11
CQ-19	69.2	8.22	201	25.5	0.77	0.85	0.08	1.16	1.23	0.88	0.63
CQ-21	75.5	7.71	212	21.3	0.85	0.88	0.13	1.1	1.18	0.84	0.59
CQ-23	73.9	6.23	226	45.8	0.68	0.88	0.08	2.86	2.02	0.67	0.82
CQ-24	76.7	4.57	114	56.8	0.64	0.9	0.08	1.74	1.07	1.37	0.86
CQ-26	76.8	4.78	182	24	0.85	0.92	0.22	1.24	0.71	1.52	0.71
CQ-28	81.3	2.3	42.8	51.8	0.78	0.96	0.15	1.14	0.88	1.56	1.06
CQ-29	87.5	3.71	74.3	63.6	0.74	0.94	0.07	2.85	1.32	1.25	0.92
CQ-30	82.5	6.99	177	52.6	0.78	0.89	0.02	3.3	2.55	0.62	0.61
CQ-31	88.6	3.48	80.5	63.2	0.6	0.93	0.08	3.02	1.32	1.26	0.9
CQ-32	88.5	3.74	88.4	58.8	0.66	0.93	0.04	3.1	1.31	1.25	0.87
CQ-33	91.6	2.84	99.2	57.9	0.72	0.95	0.01	3.08	1.29	1.26	0.88
CQ-51	74.1	3.59	135	68.7	0.78	0.93	0.16	4.69	1.32	1.2	0.88
NS-70	70.7	3.61	57.4	37.4	0.6	0.91	0.04	0.9	1.14	1.02	0.91
NS-67	67.2	5	67.7	40.4	0.67	0.89	0.06	1.09	1.55	0.78	0.82
NS-37	70.7	10.4	145	26.6	0.71	0.81	0.03	0.67	1.18	1.01	0.59
NS-34	70.3	9.45	99.7	31.3	0.76	0.83	0.08	1.03	1.23	0.85	0.59
NS-27	70.6	7.93	136	31.1	0.67	0.84	0	0.93	1.04	0.94	0.87
NS-23	81.3	2.67	168	30.6	0.7	0.95	0.13	0.88	1.1	0.89	0.8
NS-22	65.5	2.99	88.7	39.1	0.7	0.93	0.53	0.63	1.69	0.7	0.97
NS-20	69.9	2.71	30.4	42.1	0.71	0.94	0.14	0.44	1.2	0.99	0.9
NS-18	78.3	5.90	58.2	33.3	0.7	0.89	0.05	0.83	1.37	0.8	0.71
NS-17	77	5.85	163	24.1	0.77	0.9	0.15	0.89	1.04	0.93	0.55
NS-16	78.8	5.63	89.7	30.1	0.78	0.91	0.17	1.3	1.27	0.88	0.63
NS-14	77	6.04	55.7	30.5	0.76	0.9	0.08	0.87	1.23	0.89	0.57
NS-13	76	8.88	153	29.3	0.79	0.86	0.07	1.46	1.09	0.95	0.48
NS-12	76.9	5.81	167	23.1	0.72	0.89	0.07	1.21	1.02	0.97	0.45
NS-11	80.3	5.01	121	24.5	0.68	0.91	0.01	0.59	0.99	0.9	0.51
NS-10	78.7	5.19	20.1	30.7	0.73	0.91	0.06	0.36	1.02	1.01	1.08
NS-9	81.6	5.98	86.6	25	0.76	0.9	0	0.66	1.32	0.79	0.6
NS-7	89.3	2.44	25.8	35.6	0.73	0.96	0.42	0.42	1.11	1.01	1.02
NS-6	83.5	2.9	27.2	32.5	0.71	0.95	0.2	0.55	1.12	1.01	1.04
NS-5	83.5	2.9	68.9	32.1	0.74	0.95	0.28	0.81	1.58	0.72	0.9
NS-4	78.1	3.35	51.9	32.7	0.73	0.94	0.49	0.62	1.24	0.9	1
NS-3	87.3	3.5	21.1	29.6	0.72	0.94	0.36	0.5	1.14	0.99	1.05
NS-2	68.8	8.14	71.7	33.3	0.61	0.82	0.05	0.98	1.37	0.8	0.75
NS-1	87	2.68	19.7	27.2	0.7	0.95	0.64	0.64	0.97	1.03	0.87

Note that CC, CQ, and NS represent the Caicun, Changqiao, and Niushan section, respectively

Jiang et al. 1993; Van den Boorn et al. 2010). Biogenic cherts are first recorded in the Paleozoic (Qiu and Wang 2011); however, the geochemical signature of cherts of the Da-long Formation in the Upper Yangtze region indicates that their Si was derived from hydrothermal activity (Zeng et al. 2004; Chen et al. 2012). It is quite possible that cherts deposited in different regions during the same period have different origins.

Major-element analysis can be used to distinguish the origin of cherts influenced by hydrothermal activity. These are enriched in Fe and Mn (Yamamoto 1987). The Al content is considered to vary with siliciclastic input (Boström et al. 1973). An Al/(Al + Fe + Mn) value of > 0.6 indicates a biogenic origin, whereas a value of < 0.01 indicates a hydrothermal origin (Yamamoto 1987). In the present study, the Al/(Al + Fe + Mn) values of all samples of chert from southern Anhui Province are > 0.6, suggesting that their silica was derived from siliceous marine organisms.

An Al–Fe–Mn triangular plot of chert compositions can be used to identify the source of silica (Adachi et al. 1986). However, the signal of a hydrothermal contribution can be overprinted by an influx of siliciclastic material (Chen et al. 2012). Therefore, both Al–Fe–Mn and Al_{xs}–Fe_{xs}–Mn_{xs} (Al-normalized) diagrams are used here to determine the origin of silica in chert. The results shown in Fig. 5 reveal no obvious distinction between the Al–Fe–Mn and Al_{xs}–Fe_{xs}–Mn_{xs} (Al-normalized) diagrams, indicating that the cherts were deposited in a non-hydrothermal environment.

In their study on Paleozoic cherts in eastern Australia, Aitchison and Flood (1990) claimed that the ratio of Si/(Si + Fe + Al) can be used to determine the origin of cherts. Their results show that biogenic cherts mostly have a high Si/(Si + Fe + Al) value (> 0.9). The average Si/(Si + Fe + Al) value in the present study is 0.9 (Table 1), providing more evidence of a biogenic origin. In addition, the Eu* (Eu anomaly) of cherts analyzed in this study varies from 0.45 to 1.37 (mean = 0.83), indicating that the Da-long Formation cherts were not influenced by hydrothermal activity during their formation (Murray et al. 1991).

The Da-long Formation cherts may have been influenced by terrigenous detrital input, resulting in further changes in mineral compositions, such as high concentration of detrital quartz, clays, and hematite. Generally speaking, the solubility of Al and Ti is very low in seawater and they are immobile during diagenesis, while detrital sources contain high amounts of Al and Ti. Thus, aluminum or titanium

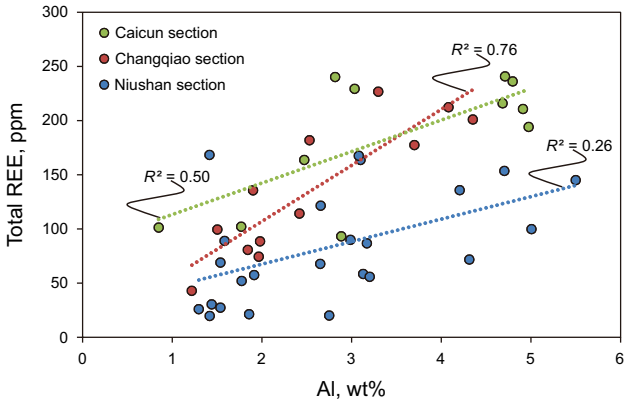

Fig. 6 Plot of chert total REE composition against Al composition

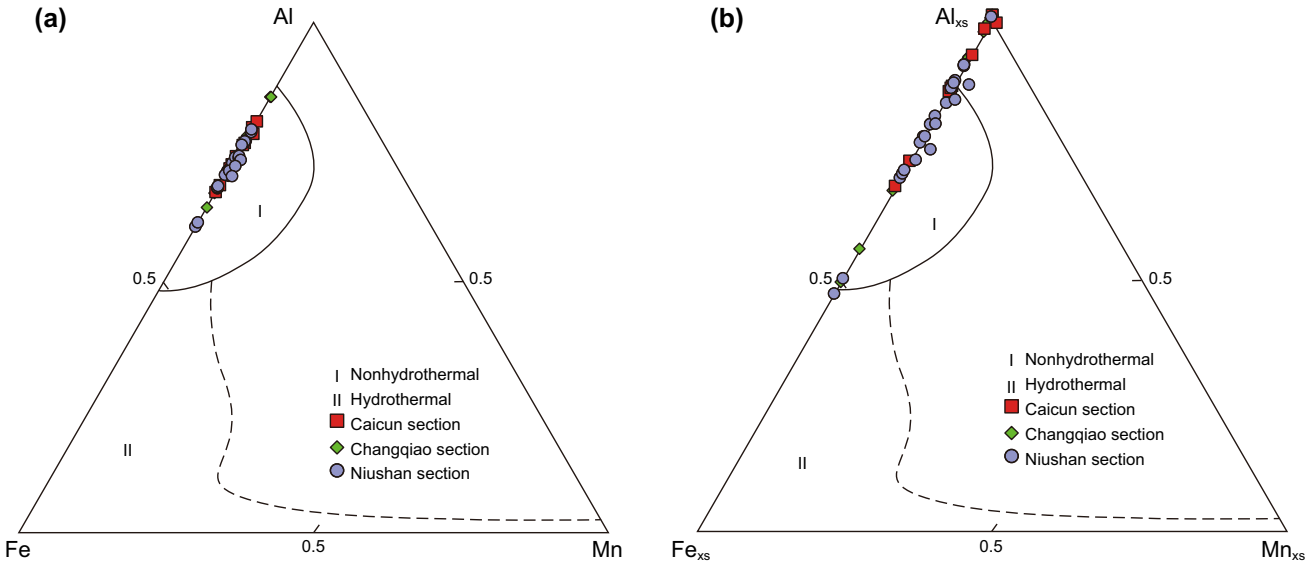

Fig. 5 Al–Fe–Mn diagram (**a**) and Al_{xs}–Fe_{xs}–Mn_{xs} (Al-normalized) diagram (**b**) for the thin-bedded cherts of the Da-long Formation. Hydrothermal and non-hydrothermal fields are from Adachi et al. (1986)

commonly represents a detrital origin (Tribovillard et al. 2006). Rocks that contain high concentrations of Al_2O_3 and TiO_2 indicate they are strongly influenced by detrital input. The Al_2O_3 content of the cherts (mean = 5.42 wt%) is much less than the 18.09 wt% of the PAAS (Post Archean Australia Shales; Taylor and McLennan 1985) standard, but is higher than typical biological cherts in the open ocean (0.71 wt%; Hein et al. 1981). Similarly, the TiO_2 content of the Da-long cherts (mean = 0.17 wt%) is higher than that of typical biogenic cherts (0.03 wt%; Hein et al. 1981). Interestingly, there is a strong correlation between Al_2O_3 and ΣREE in the Da-long Formation cherts (Fig. 6). This relationship shows that the contribution of terrigenous detrital sediment is important, particularly in the Changqiao section ($R^2 = 0.76$) (Fig. 6). Some samples have a relatively low Al_2O_3 content (e.g., CC-10, at 1.60 wt%), which implies that some areas at the northern margin of Yangtze region have little input of continental detritus from the South China Block and North China Block (Wu 1999). In conclusion, the geochemical data from this study [including Al/(Al + Fe + Mn), Al_{xs}–Fe_{xs}–Mn_{xs}, and Si/(Si + Fe + Al) data, and Eu anomalies] show that the siliceous rocks are primarily biological in origin, with some continental detrital input, but with no hydrothermal contribution. This view is supported by the presence of round radiolarians, sponge spicules, and other siliceous debris in the cherts (Fig. 4).

5.2 Sedimentary environment

Siliceous rocks occur in a range of depositional environments such as continental margins and deep-water basins. The sedimentology of cherts can therefore provide valuable paleoceanographic information (Murchey and Jones 1992). It is generally acknowledged that the Mn content of siliceous rocks represents the influence of hydrothermal activity and that Ti, which has a low solubility in seawater, is considered to indicate a terrestrial input. Thus, the ratio of Mn/Ti can be used to distinguish the sedimentary environment of siliceous rocks. According to synthetic studies by Boström et al. (1973) and Adachi et al. (1986), the Mn/Ti ratio of siliceous rocks deposited in open marine conditions is > 0.5, with a value of < 0.5 indicating continental slope or marginal marine settings. The Mn/Ti ratios of the Da-long Formation cherts vary from 0.005 to 0.64 (mean = 0.14), with only two samples (NS-22 and NS-102) yielding values greater than 0.5 (Table 1). Therefore, the Da-long Formation cherts are inferred to have been deposited in a continental slope or marginal marine environment, rather than in open water.

The REE compositions of chert and shale can indicate the depositional environment (Murray et al. 1990). For example, the Ce anomaly can be used to identify the relative distance from terrestrial sediment input. Murray et al. (1990, 1991) studied the Ce anomaly of cherts collected from the Franciscan Complex in California, which yields mean values of 0.29 at a spreading ridge, 0.6 in an ocean-basin setting, and 0.9–1.30 at a continental margin. In addition to the Ce anomaly, the La_N/Ce_N ratio is a useful indicator of the sedimentary environment. Statistical analysis has revealed that cherts deposited at a continental margin yield a La_N/Ce_N ratio near to 1, whereas those deposited at a spreading ridge or a pelagic environment yield values greater than 3.5 and 2–3, respectively (Murray 1994).

A comparison of the $Al_2O_3/(Al_2O_3 + Fe_2O_3)$, La_N/Ce_N, and Fe_2O_3/TiO_2 ratios of cherts can indicate the sedimentary environment. Cherts deposited in a continental margin environment with significant terrigenous input generally yield $Al_2O_3/(Al_2O_3 + Fe_2O_3)$ values of > 0.50 and Fe_2O_3/TiO_2 values of < 50. Those deposited in an ocean basin, far

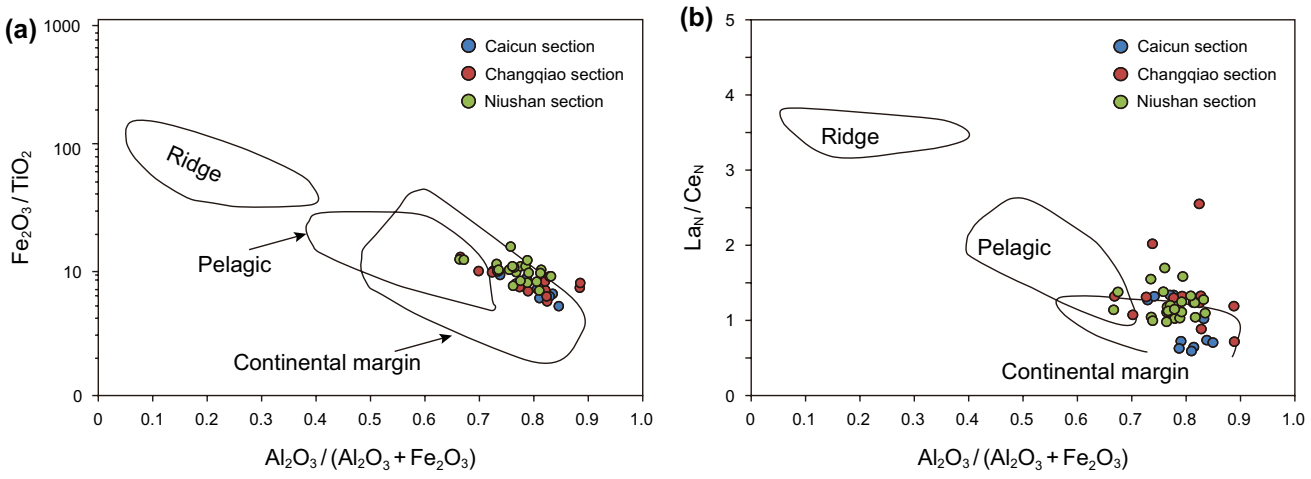

Fig. 7 Chert $Al_2O_3/(Al_2O_3 + Fe_2O_3)$ versus Fe_2O_3/TiO_2 (**a**) and La_N/Ce_N (**b**) diagrams. The ridge, pelagic, and continental margin fields are from Murray (1994)

from continental input but near to a region of hydrothermal activity, yield $Al_2O_3/(Al_2O_3+Fe_2O_3)$ values of <0.50 and Fe_2O_3/TiO_2 values of >50 (Fig. 7).

The Ce anomaly of the Da-long Formation cherts varies from 0.62 to 1.86 (mean = 1.06) (Table 1), indicating that the cherts were deposited in an area between the continental margin and an ocean basin. Moreover, the Changqiao and Caicun sections are closer to a terrestrial source. The La_N/Ce_N results show that the cherts do not belong to the three typical sedimentary environments mentioned above, but instead indicate a transitional zone between a continental margin and a pelagic depositional environment. The Y/Ho values of the Da-long Formation cherts (mean = 35) range from the value of PAAS (27.3) to that of modern seawater (55; Nozaki et al. 1997), suggesting their formation from seawater with terrestrial input. The geochemical data of the present study are supported by the paleogeographic research of Feng et al. (1993), who showed that the Lower Yangtze Sea was located in the northwestern part of the Zhejiang–Fujian–Guangdong clastic region during the late Permian (Fig. 1b). This explains why the sediments from the Changqiao and Caicun sections have a large terrestrial input.

In conclusion, we suggest that the black bedded siliceous rocks of the Da-long Formation in the Lower Yangtze region were deposited mainly at a continental margin and received some terrestrial sediment input, but were far from sites of hydrothermal activity.

5.3 Chert Formation

Detailed field work and thin-section observations of the three studied sections reveal that the upper Permian Da-long Formation records a marine transgression–regression cycle (Zhu et al. 1989; Liao et al. 2016a). The thin-bedded cherts were deposited during the transitional period of this sea-level cycle, which represents the greatest water depth in the Yangtze Sea (Tian et al. 2007; Li et al. 2009; Qiu and Wang 2011). At this time, the northern margin of the Yangtze basin encompassed the region from the continental margin to an oceanic basin. The geochemical and sedimentological characteristics of the 47 thin-bedded black siliceous rocks examined in this study support the interpretation of a deep-water and anoxic oceanic environment during the late Permian (Wu et al. 1994).

During the late Permian, South China was located at a low latitude, in a tropical climate zone (Yin et al. 1999). This environment was characterized by a hot climate and relatively high primary productivity (Shen et al. 2014), which is favorable for siliceous zooplankton to flourish. Furthermore, the Paleo-Tethys Sea was marked by intense upwelling at its eastern margin due to its paleogeographic position (Kidder and Worsley 2004). The upwelling would have brought an abundance of nutrients such as Si, Mo, Ni, Cu, Zn, and P toward the surface.

The nutrient- and silicon-rich surface water would have favored siliceous and other biological organisms, and could have accelerated Si precipitation through the mixing of cold and hot water or via biological accumulation (e.g., Kametaka et al. 2005; Bai et al. 2008; Feng and Algeo 2014). The sedimentary deposits associated with this upwelling contain abundant silicon- or phosphorus-rich organisms and show anoxic characteristics such as the absence of benthos and a lamellar structure (Wang 1993; Wu et al. 1994; Lü et al. 2004). Bedded cherts produced by upwelling are widely distributed in the Yangtze Block, such as in the upper Permian Gufeng Formation (Kametaka et al. 2005). Even the Phosphoria Formation in North America (Murchey and Jones 1992) and upper Permian strata of the Sverdrup Basin (Arctic Canada) are considered to be related to upwelling (Beauchamp and Grasby 2012).

Regional volcanism may also influence the formation of cherts. As shown in Fig. 3b, there are many volcanic ash layers within the Caicun section (up to 15). In fact, such layers are common not only in the three studied sections but also in the South China or Paleo-Tethys region (e.g., Shen et al. 2012; Yin et al. 1992; Liao et al. 2016b). Petrological and mineralogical evidence indicates that the ash layers were derived from the alteration of volcanic materials produced by felsic volcanism (e.g., Liao et al. 2016b). Abundant tephra particles are found in siliceous rocks of the Da-long Formation in southern Anhui Province (Zhu et al. 1989). This suggests that the formation of cherts is controlled by regional volcanism to some extent. Note that there is little definite evidence of volcanic ash in the Boreal realm (Grasby et al. 2015), different from the case of this study. This implies that chert formation might not have a strong relation with volcanism in a global perspective. Thus, the influence of volcanism on the formation of chert in the Paleo-Tethys Ocean may only be a regional event. The submarine weathering of volcanic ash would increase the nutrient flux (e.g., P, Ba, Cu, Zn, Ni, and Cd). These elements are essential to all forms of life on Earth, as they play a fundamental role in many metabolic processes and are a constituent of skeletal material (Tribovillard et al. 2006). Abundant nutrient flux is favorable for the flourishing of siliceous zooplankton. With the sinking of silica-rich organisms, siliceous sediments can be produced. Moreover, it has been reported that silica from volcanic ash promotes Si precipitation in seawater (Kong and Gong 1986). Silica-rich organisms absorb the volcanogenic silicon through their metabolism in warm surface waters (Kong and Gong 1986). Thus, the accumulation of siliceous skeletal material leads to the formation of radiolarian-bearing thin-bedded cherts (Fig. 8). In summary, intense regional volcanism can accelerate the formation of siliceous

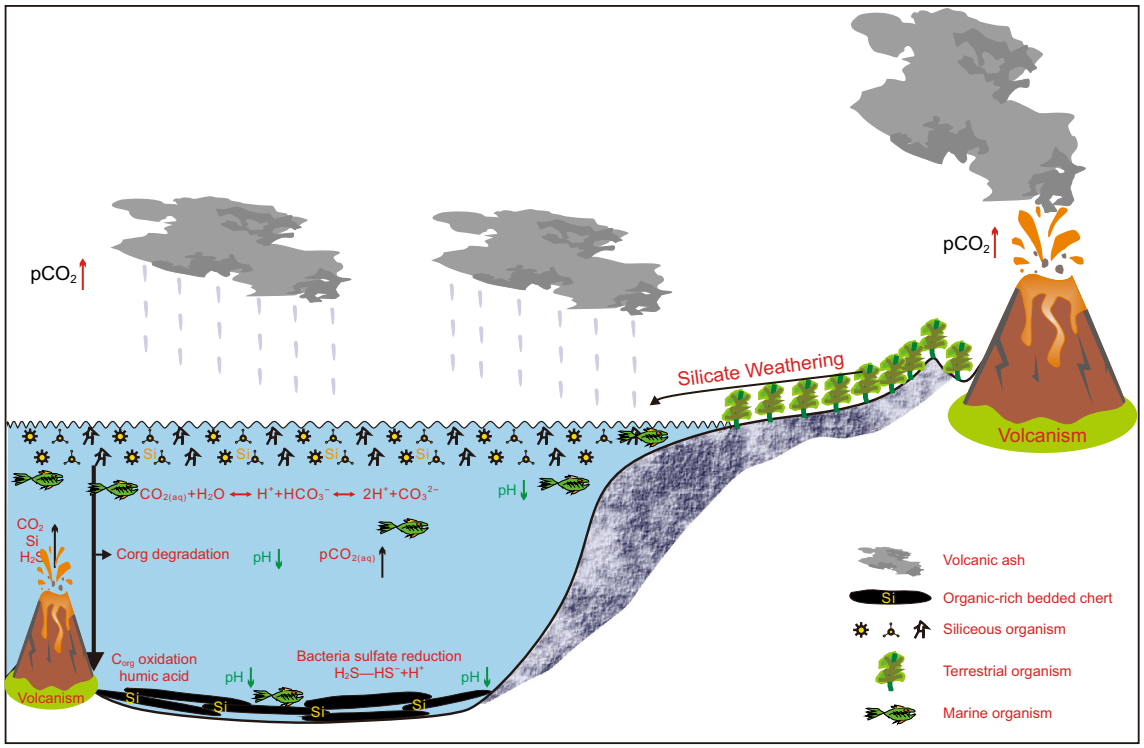

Fig. 8 Model of the formation of the Da-long Formation bedded cherts

deposits, yet the silica in cherts is not directly formed from volcanism or hydrothermal activity.

Although the occurrence of radiolarian in the Da-long Formation shows it is of biological origin, the evidence of major and trace elements from siliceous rocks (e.g., Shangsi) containing abundant silica-rich organisms suggests a hydrothermal origin. As a result, the comprehensive measures of traditional observations and geochemistry are more sensitive to detect hydrothermal signals. The geochemical data reported here show that the cherts are biological rather than hydrothermal in origin. However, several other sections of the Da-long Formation in South China are related to hydrothermal activity. For example, cherts in the Chongyang section at Hubei and the Tongling section at Anhui are thought to have been formed in association with a fracture system (Cheng et al. 2015). The latter section is near to the present study area, and here the hydrothermal cherts were deposited in association with the formation of molybdenum ore (Zeng et al. 2004). Despite this, our data indicate that the influence of hydrothermal activity was relatively limited.

Siliceous rocks of the Da-long Formation in South China are mainly of biological origin, with those of hydrothermal origin being less than 30% of samples studied (Table 2) and distributed only locally. The ocean chemistry and the effects of local volcanism are the main factors that control the sedimentology of thin-bedded siliceous rocks. All kinds of volcanic-hydrothermal systems occurred globally during the late Permian (Veevers and Tewari 1995), whereas the volcanism in the South China block was relatively far from the sedimentary depocenter (Liao et al. 2016b). Therefore, volcanic-hydrothermal activity did not have a direct effect on the genesis of the Da-long Formation cherts in most regions, although some areas may have been influenced by a deep fault system (Qiu and Wang 2011; Chen et al. 2012).

5.4 Implications for the late Permian marine environment

The Permian was a special period in the earth's history (Yin and Song 2013). Co-incident with the formation of the supercontinent of Pangea in the late Permian (Golonka et al. 1994) are siliceous sediments that are widespread around the globe. Permian siliceous rocks from the circum-Pacific and Mediterranean regions reveal a widespread Permian Chert Event (PCE) during the middle Leonardian to Wordian (Murchey and Jones 1992), which may have lasted as long as 30 Myr (Beauchamp and Baud 2002). In fact, cherts and siliceous rocks occur in multiple locations in South China during every stage of the Permian (Yao et al. 2013), with a peak in chert occurrence during the Guadalupian and Changhsingian stages.

The Da-long Formation bedded cherts are part of the PCE, indicating unusual global paleoceanographic conditions at this time. Silica precipitation requires suitable physical and

Table 2 Summary of published research on the origin of the Da-long Formation siliceous rocks in South China

No.	Section or location	Region	Evidence	Paleoredox conditions	Siliceous source	References
1	Guangyuan, Enshi, Chaohu and Guchi sections, northern margin of Yangtze platform	Upper, Middle and Lower Yangtze region	Major and trace metal element	–	Biogenic	Cheng et al. (2015)
2	Daye, Changyang and Tongling sections, southern Hubei and Anhui Province	Middle Yangtze region	Major and trace metal element	–	Primarily biogenic, some hydrothermal	Cheng et al. (2015)
3	Chaohu and Chaoqiao section at southern Anhui Province	Lower Yangtze region	Major and trace metal element	Anoxic	Biogenic	Li et al. (2015)
4	Huangshi section, southeastern Hubei Province	Middle Yangtze region	Major and trace metal element, Si and O isotopes	Dysoxic/oxic	Hydrothermal	Xu (1997)
5	Tongling section, southern Anhui Province	Middle Yangtze region	Major and trace metal element	Oxic	Hydrothermal	Zeng et al. (2004)
6	Zhaojieba section, western Hubei Province	Middle Yangtze region	Major and trace metal element	Euxinic	Biogenic	Yu et al. (2012)
7	Zhaoguya section, western Hubei Province	Middle Yangtze region	Major and trace metal element	Euxinic	Primarily biogenic, some hydrothermal	Lei et al. (2002)
8	Multiple sections at Hunan and Guizhou and Guangxi Province	Upper Yangtze region	Major and trace metal element	–	Primarily biogenic	Qiu and Wang (2010)
9	Multiple sections at Laibin, Bama and Liuzhou in Guangxi Province	Upper Yangtze region	Major and trace metal element	–	Hydrothermal	Qiu and Wang (2010, 2011)
10	Shangsi section, northeastern Sichuan Province	Upper Yangtze region	Major and trace metal element	Anoxic	Primarily biogenic, some hydrothermal	Chen et al. (2012)
11	Shangsi section, northeastern Sichuan Province	Upper Yangtze region	Major and trace metal element	Anoxic	Primarily biogenic, some hydrothermal	Li et al. (2009)
12	Luodian section, southern Guizhou Province	Upper Yangtze region	Major and trace metal element	–	Primarily biogenic, some hydrothermal	Li et al. (2009)
13	Dongpan section, Guangxi Province	Upper Yangtze region	Major and trace metal element	Oxic	Biogenic	Tian et al. (2007)
14	Chaohu section, southern Anhui Province	Lower Yangtze region	Sedimentary features	Anoxic	Biogenic	Zhu et al. (1989)

chemical conditions, including temperature, pressure, pH, and seawater silica content (Hesse 1989). The pH of marine waters is vital for the preservation of siliceous sediments in the rock record. Beauchamp and Grasby (2012) and Grasby et al. (2015) suggested that lysocline shoaling and ocean acidification along northwest Pangea led to carbonate dissolution and chert expansion during the late Permian (i.e., Canadian Arctic Islands and Spitzbergen). The global atmospheric CO_2 content (7%–8%) was high during the late Permian (Berner 2002), which would have enhanced continental weathering. In this case, the input of abundant terrestrial silica and other nutrients into seawater would have enhanced biological

production. Simultaneously, elevated atmospheric CO_2 levels would have increased the partial pressure of carbon dioxide in surface seawater $CO_{2(aq)}$. Accordingly, some marine organisms (e.g., calcareous algae and foraminifera) would have been confronted with severe environmental stress triggered by a low global ocean pH (Clapham and Payne 2011). However, siliceous marine biota can thrive in an acidified ocean and rapidly bloom in a stress-free environment. This explains how an abundance of siliceous biota became the main source of silicon in the formation of the thin-bedded siliceous rocks of the Da-long Formation.

The decay of organic-rich siliceous organisms consumes a large amount of free oxygen in seawater, which results in the underlying water becoming hypoxic. This process releases CO_2 (Fig. 8) into seawater, increasing its CO_2 concentration. With the sinking of organic matter, further decomposition within the sediment during the bacterial sulfate reduction (BSR) stage would give rise to anaerobic/anoxic conditions. Several lines of evidence can confirm the BSR may occur in siliceous rocks. Firstly, the pyrites in cherts are lamellar (Fig. 3c) and framboidal (Fig. 4l), suggesting an authigenic origin related to BSR (Lang et al. 2018). Secondly, $\delta^{34}S_{py}$ values range from − 41.20 to − 19.70‰ (unpublished data), all of which are obviously lower than the $\delta^{34}S$ value (approximately + 10‰) of seawater sulfate in the late Permian (Strauss 1997); thus, fractionation of − 51.20‰ to + 29.70‰ occurred. Such high fractionation of $\delta^{34}S_{py}$ suggests that those pyrite may formed by BSR (Machel 2001). CO_2 would be liberated into seawater by local submarine magmatism, changing the chemistry of seawater and reducing the pH, with acidic conditions favoring the preservation of siliceous rock. In addition, the expulsion of hydrocarbons from the decay of organic matter releases organic acids into seawater during the early stage of diagenesis. This process also lowers the pH of the water and favors silica preservation (Williams and Crerar 1985).

Global ocean acidification occurred during the late Permian (e.g., Knoll et al. 2007; Kroeker et al. 2010; Hinojosa et al. 2012), and this has been proposed as a cause of the PTB mass extinction, triggered by large-scale volcanism and the release of large volumes of volcanic CO_2 (Clarkson et al. 2015). The PCE might have been indirectly linked to some extent to many contemporary volcanic episodes, such as the Emeishan basalts in South China (Sun et al. 2010), the Siberian flood basalts (Reichow et al. 2009), and local felsic volcanism (Liao et al. 2016b).

6 Conclusions

In this study, detailed sedimentological observations and geochemical data were used to assess the origin of the upper Permian Da-long Formation siliceous rocks in the Lower Yangtze region (southeastern China), and their implications for Permian ocean chemistry. The main conclusions are as follows.

1. The geochemical characteristics of the siliceous rocks of the Da-long Formation indicate that they had a biological origin, with some terrigenous detrital input. The cherts were deposited in a transitional environment between the continental margin and a deep oceanic basin, far from hydrothermally active regions.
2. The late Permian thin-bedded cherts of the Yangtze region were deposited as part of a global Permian Chert Event. Intense volcanism in the Paleo-Tethyan region and nutrient upwelling at this time were the main controlling factors that explain the high productivity of silicic biota and silica precipitation in the study area. The contemporaneous ocean acidification event provided favorable chemical conditions for silica preservation.

Acknowledgements We thank Associate Editor Dr. Meijun Li and two anonymous reviewers for the constructive comments and suggestions, which helped to improve the article. This study was jointly supported by the National Natural Science Foundation of China (Grant No. 41702129), Chongqing Research Program of Basic Research and Frontier Technology (Grant No. cstc2017jcyjAX0448), Open Fund of Key Laboratory of Sedimentary Basin and Oil and Gas Resources, Ministry of Land and Resources (Chengdu Center, CGS) (Grant No. CDCGS2018003), State Key Laboratory of Palaeobiology and Stratigraphy (Nanjing Institute of Geology and Palaeontology, CAS) (Grant No. 173115), the Science and Technology Research Program of Chongqing Municipal Education Commission (Grant No. KJQN201800115), and of Fundamental Research Funds for the Central Universities (Grant No. 106112017CDJXY240001).

References

Adachi M, Yamamoto K, Sugisaki R. Hydrothermal chert and associated siliceous rocks from the northern Pacific: their geological significance as indication of ocean ridge activity. Sediment Geol. 1986;47:125–48. https://doi.org/10.1016/0037-0738(86)90075-8.

Aitchison JC, Flood PG. Geochemical constraints on the depositional setting of Palaeozoic cherts from the New England orogen, NSW, eastern Australia. Mar Geol. 1990;94(1):79–95. https://doi.org/10.1016/0025-3227(90)90104-R.

Anhui Provincial Geological Bureau. The Regional Geology of Anhui Province. Beijing: Geological Publishing House; 1987. p. 1–247 **(in Chinese)**.

Bai X, Luo GM, Wu X, et al. Carbon isotope records indicative of paleoceanographical events at the latest Permian Dalong formation

at Shangsi, northeast Sichuan, China. J China Univ Geosci. 2008;19(5):481–7. https://doi.org/10.1016/S1002-0705(08)60053-9.

Bates RL, Jackson JA. Glossary of geology. 2nd ed. Falls Church: American Geological Institute; 1980. p. 1–751.

Beauchamp B, Baud A. Growth and demise of Permian biogenic chert along northwest Pangea: evidence for end-Permian collapse of thermohaline circulation. Palaeogeogr Palaeoclimatol Palaeoecol. 2002;184(1–2):37–63. https://doi.org/10.1016/S0031-0182(02)00245-6.

Beauchamp B, Grasby SE. Permian lysocline shoaling and ocean acidification along NW Pangea led to carbonate eradication and chert expansion. Palaeogeogr Palaeoclimatol Palaeoecol. 2012;350–352(1):73–90. https://doi.org/10.1016/j.palaeo.2012.06.014.

Berner RA. Examination of hypotheses for the Permo–Triassic boundary extinction by carbon cycle modeling. Proc Natl Acad Sci USA. 2002;99:4172–7. https://doi.org/10.1073/pnas.032095199.

Boström K, Kraemer T, Gartner S. Provenance and accumulation rates of opaline silica, Al, Ti, Fe, Mn, Cu, Ni and Co in Pacific pelagic sediments. Chem Geol. 1973;11(2):123–48. https://doi.org/10.1016/0009-2541(73)90049-1.

Cao TT, Song ZG, Wang SB, et al. Physical property characteristics and controlling factors of Permian shale reservoir in the Lower Yangtze platform. Nat Gas Geosci. 2015;26(2):341–51. https://doi.org/10.11764/j.issn.1672-1926.2015.02.0341 **(in Chinese)**.

Chen DZ, Qing HR, Yan X, et al. Hydrothermal venting and basin evolution (Devonian, South China): constraints from rare earth element geochemistry of chert. Sediment Geol. 2006;183(3):203–16. https://doi.org/10.1016/j.sedgeo.2005.09.020.

Chen H, Xie XN, Hu CY, et al. Geochemical characteristics of Late Permian sediments in the Dalong Formation of the Shangsi Section, Northwest Sichuan Basin in South China: implications for organic carbon-rich siliceous rocks formation. J Geochem Explor. 2012;112(1):35–53. https://doi.org/10.1016/j.gexplo.2011.06.011.

Cheng C, Li SY, Zhao DQ, et al. Geochemical characteristics of the Middle-Upper Permian bedded cherts in the northern margin of the Yangtze block and its response to the evolution of paleogeography and paleo-ocean. Bull Mineral Pet Geochem. 2015;34(1):155–66. https://doi.org/10.3969/j.issn.1007-2802.2015.01.018 **(in Chinese)**.

Clapham ME, Payne JL. Acidification, anoxia, and extinction: a multiple logistic regression analysis of extinction selectivity during the Middle and Late Permian. Geology. 2011;39(11):1059–62. https://doi.org/10.1130/G32230.1.

Clarkson MO, Kasemann SA, Wood RA, et al. Ocean acidification and the Permo–Triassic mass extinction. Science. 2015;348(6231):229–32. https://doi.org/10.1126/science.aaa0193.

Du YL, Li SY, Kong WL, et al. The Permian sedimentary facies and depositional environment analysis in the Jingxian–Nanling region of Anhui. J Stratigr. 2010;4:431–44 **(in Chinese)**.

Fan HF, Wen HJ, Zhu XK, et al. Hydrothermal activity during Ediacaran–Cambrian transition: silicon isotopic evidence. Precambrian Res. 2013;224(224):23–35. https://doi.org/10.1016/j.precamres.2012.09.004.

Feng QL, Algeo TJ. Evolution of oceanic redox conditions during the Permo–Triassic transition: evidence from deepwater radiolarian facies. Earth Sci Rev. 2014;137:34–51. https://doi.org/10.1016/j.earscirev.2013.12.003.

Feng QL, Gu SZ. Uppermost Changxingian (Permian) radiolarian fauna from southern Guizhou, southwestern China. J Paleontol. 2002;76:797–809. https://doi.org/10.1017/S0022336000037483.

Feng ZZ, He YB, Wu SH. Lithofacies paleogeography of Permian middle and Lower Yangtze Region. Acta Sedimentol Sin. 1993;3:12–24. https://doi.org/10.14027/j.cnki.cjxb.1993.03.003 **(in Chinese)**.

Gao JF, Lu JJ, Lai MY, et al. Analysis of trace elements in rock samples using HR-ICPMS. J Nanjing Univ (Nat Sci). 2003;39(6):844–50 **(in Chinese)**.

Golonka J, Ross MI, Scotese CR. Phanerozoic paleogeographic and paleoclimatic modeling maps. Can Soc Pet Geol Mem. 1994;17:1–47.

Grasby SE, Beauchamp B, Bond DPG, et al. Progressive environmental deterioration in northwestern Pangea leading to the latest Permian extinction. GSA Bull. 2015;127(9–10):1331–47. https://doi.org/10.1130/B31197.1.

Han SC, Hu K, Cao J, et al. Origin of early Cambrian black-shale-hosted barite deposits in South China: mineralogical and geochemical studies. J Asian Earth Sci. 2015;106:79–94. https://doi.org/10.1016/j.jseaes.2015.03.002.

Hein JR, Vallier TL, Allan MA. Chert petrology and geochemistry, mid-Pacific Mountains and Hess Rise, Deep Sea Drilling Project Leg 62. In: Thiede J, Vallier TL, et al., editors. Initial reports of the DSDP, vol. 62. Washington: U.S. Government Printing Office; 1981. p. 711–48.

Hesse R. Silica diagenesis: origin of inorganic and replacement cherts. Earth Sci Rev. 1989;26(1):253–84. https://doi.org/10.1016/0012-8252(89)90024-X.

Hinojosa JL, Brown ST, Chen J, et al. Evidence for end-Permian ocean acidification from calcium isotopes in biogenic apatite. Geology. 2012;40(8):743–6. https://doi.org/10.1130/G33048.1.

Hu G, Hu WX, Cao J, et al. The distribution, hydrocarbon potential, and development of the Lower Cretaceous black shales in coastal southeastern China. J Palaeogeogr. 2017;6(4):333–51. https://doi.org/10.1016/j.jop.2017.08.002.

Jiang SY, Ding TP, Wan DF, et al. Silicon isotopic compositions of Archean banded Si–Fe formation (BIF) in the Gongchangling ore deposit, Liaoning Province, China. Sci China Ser B. 1993;36(4):482–9.

Jones DL, Murchey B. Geologic significance of Paleozoic and Mesozoic radiolarian chert. Annu Rev Earth Planet Sci. 1986;14(1):455–92. https://doi.org/10.1146/annurev.ea.14.050186.002323.

Kametaka M, Takebe M, Nagai H, et al. Sedimentary environments of the Middle Permian phosphorite–chert complex from the northeastern Yangtze platform, China; the Gufeng Formation: a continental shelf radiolarian chert. Sediment Geol. 2005;174(3–4):197–222. https://doi.org/10.1016/j.sedgeo.2004.12.005.

Kato Y, Nakao K, Isozaki Y. Geochemistry of Late Permian to Early Triassic pelagic cherts from southwest Japan: implications for an oceanic redox change. Chem Geol. 2002;182(1):15–34. https://doi.org/10.1016/S0009-2541(01)00273-X.

Kidder DL, Worsley TR. Causes and consequences of extreme Permo–Triassic warming to globally equable climate and relation to the Permo–Triassic extinction and recovery. Palaeogeogr Palaeoclimatol Palaeoecol. 2004;203(3):207–37. https://doi.org/10.1016/S0031-0182(03)00667-9.

Knoll AH, Bambach RK, Payne JL, et al. Paleophysiology and end-Permian mass extinction. Earth Planet Sci Lett. 2007;256:295–313. https://doi.org/10.1016/j.epsl.2007.02.018.

Kong QY, Gong YJ. Origin of the lower Permian siliceous rocks in Chaoxian County, Anhui. Oil Gas Geol. 1986;7(2):171–4 **(in Chinese)**.

Kroeker KJ, Kordas RL, Crim RN, et al. Meta-analysis reveals negative yet variable effects of ocean acidification on marine organisms. Ecol Lett. 2010;13:1419–34. https://doi.org/10.1111/j.1461-0248.2010.01518.x.

Lang XG, Shen B, Peng YB, et al. Transient marine euxinia at the end of the terminal Cryogenian glaciation. Nat Commun. 2018;9:3019. https://doi.org/10.1038/s41467-018-05423-x.

Lei BJ, Que HP, Hu N, et al. Geochemistry and sedimentary environments of the Palaeozoic siliceous rocks in western Hubei. Sediment Geol Tethyan Geol. 2002;22(2):70–9 **(in Chinese)**.

Li HJ, Lin ZL, Xie XN. Geochemical characteristics and origin of Palaeozoic siliceous rocks in Lower Yangtze area. Lithol Reserv. 2015;27(5):232–9 **(in Chinese)**.

Li HJ, Xie XN, Lin ZL, et al. Organic matter enrichment of Dalong Formation in Guangyuan area of the Sichuan Basin. Geol Sci Technol Inf. 2009;28(2):98–103 **(in Chinese)**.

Liao ZW, Hu WX, Cao J, et al. Heterogeneous volcanism across the Permian–Triassic Boundary in South China and implications for the latest Permian mass extinction: new evidence from volcanic ash layers in the lower Yangtze region. J Asian Earth Sci. 2016a;127:197–210. https://doi.org/10.1016/j.jseaes.2016.06.003.

Liao ZW, Hu WX, Cao J, et al. Permian–Triassic boundary (PTB) in the Lower Yangtze Region, southeastern China: a new discovery of deep-water archive based on organic carbon isotopic and U–Pb geochronological studies. Palaeogeogr Palaeoclimatol Palaeoecol. 2016b;451:124–39. https://doi.org/10.1016/j.palaeo.2016.03.004.

Lü BQ, Wang HG, Hu WS, et al. Relationship between Paleozoic upwelling facies and hydrocarbon in southeastern marginal Yangtze block. Mar Geol Quat Geol. 2004;24(4):29–35. https://doi.org/10.16562/j.cnki.0256-1492.2004.04.005 **(in Chinese)**.

Lv DW, Chen JD. Depositional environments and sequence stratigraphy of the Late Carboniferous–Early Permian coal-bearing successions (Shandong Province, China): sequence development in an epicontinental basin. J Asian Earth Sci. 2014;79:16–30. https://doi.org/10.1016/j.jseaes.2013.09.003.

Lv DW, Wang DD, Li ZX, et al. Depositional environment, sequence stratigraphy and sedimentary mineralization mechanism in the coal bed- and oil shale-bearing succession: a case from the Paleogene Huangxian Basin of China. J Pet Sci Eng. 2017;148:32–51. https://doi.org/10.1016/j.petrol.2016.09.028.

Machel HG. Bacterial and thermochemical sulfate reduction in diagenetic settings—old and new insights. Sediment Geol. 2001;140(1–2):143–75. https://doi.org/10.1016/S0037-0738(00)00176-7.

Maliva RG, Knoll AH, Siever R. Secular change in chert distribution: a reflection of evolving biological participation in the silica cycle. Palaios. 1989;4(6):519–32. https://doi.org/10.2307/3514743.

McGowran B. Silica burp in the Eocene ocean. Geology. 1989;17(9):857–60. https://doi.org/10.1130/0091-7613(1989)017%3c0857:SBITEO%3e2.3.CO;2.

Murchey BL, Jones DL. A mid-Permian chert event: widespread deposition of biogenic siliceous sediments in coastal, island arc and oceanic basins. Palaeogeogr Palaeoclimatol Palaeoecol. 1992;96(1):161–74. https://doi.org/10.1016/0031-0182(92)90066-E.

Murray RW, Buchholtz TBMR, Jones DL, et al. Rare earth elements as indicators of different marine depositional environments in chert and shale. Geology. 1990;18(3):268–71. https://doi.org/10.1130/0091-7613(1990)018%3c0268:REEAIO%3e2.3.CO;2.

Murray RW, Gerlach DC, Ten Brink MRB, et al. Rare earth, major, and trace elements in chert from the Franciscan complex and Monterey group, California: assessing REE sources to fine-grained marine sediments. Geochim Cosmochim Acta. 1991;55(7):1875–95. https://doi.org/10.1016/0016-7037(91)90030-9.

Murray RW. Chemical criteria to identify the depositional environment of chert: general principles and applications. Sediment Geol. 1994;90(3–4):213–32. https://doi.org/10.1016/0037-0738(94)90039-6.

Nozaki Y, Zhang J, Amakawa H. The fractionation between Y and Ho in the marine environment. Earth Planet Sci Lett. 1997;148:329–40. https://doi.org/10.1016/S0012-821X(97)00034-4.

Pang Q, Hu G, Jiao K, et al. Characteristics of organic pores and composition of bio-precursors in the Wufeng and Longmaxi Formation shales, Southern Sichuan Basin, China. Energy Explor Exploit. 2018;36(4):645–64. https://doi.org/10.1177/0144598717753166.

Qiu Z, Wang QC. Geochemical evidence for submarine hydrothermal origin of the Middle-Upper Permian chert in Laibin of Guangxi, China. Sci China Earth Sci. 2011;54(7):1011–23. https://doi.org/10.1007/s11430-011-4198-x.

Qiu Z, Wang QC. Geochemistry and sedimentary background of the Middle-Upper Permian cherts in the Xiang-Qian-Gui region. Acta Pet Sin. 2010;26(12):3612–28 **(in Chinese)**.

Reichow MK, Pringle MS, Al'Mukhamedovc AI, et al. The timing and extent of the eruption of the Siberian Traps large igneous province: implications for the end-Permian environmental crisis. Earth Planet Sci Lett. 2009;277(1):9–20. https://doi.org/10.1016/j.epsl.2008.09.030.

Ritterbush KA, Rosas S, Corsetti FA, et al. Andean sponges reveal long-term benthic ecosystem shifts following the end-Triassic mass extinction. Palaeogeogr Palaeoclimatol Palaeoecol. 2015;420:193–209. https://doi.org/10.1016/j.palaeo.2014.12.002.

Shen J, Algeo TJ, Hu Q, et al. Negative C-isotope excursions at the Permian–Triassic boundary linked to volcanism. Geology. 2012;40:963–6. https://doi.org/10.1130/G33329.1.

Shen J, Lian Z, Feng QL, et al. Paleo-productivity evolution across the Permian–Triassic boundary and quantitative calculation of primary productivity of black rock series from the Dalong Formation, South China. Sci China Earth Sci. 2014;57(7):1583–94. https://doi.org/10.1007/s11430-013-4780-5.

Strauss H. The isotopic composition of sedimentary sulfur through time. Palaeogeogr Palaeoclimatol Palaeoecol. 1997;132(1):97–118. https://doi.org/10.1016/S0031-0182(97)00067-9.

Shi CH, Cao J, Bao JP, et al. Source characterization of highly mature pyrobitumens using trace and rare earth element geochemistry: Sinian–Paleozoic paleo-oil reservoirs in South China. Org Geochem. 2015;83–84:77–93. https://doi.org/10.1016/j.orggeochem.2015.03.008.

Shi CH, Cao J, Tan XC, et al. Hydrocarbon generation capability of Sinian–Lower Cambrian shale, mudstone and carbonate rocks in the Sichuan Basin, southwestern China: implications for contributions to the giant Sinian Dengying natural gas accumulation. AAPG Bull. 2018;102(5):817–53. https://doi.org/10.1306/07111771417417019.

Shimizu H, Masuda A. Cerium in chert as an indication of marine environment of its formation. Nature. 1977;266(5600):346–8. https://doi.org/10.1038/266346a0.

Sun YD, Lai XN, Wignall PB, et al. Dating the onset and nature of the Middle Permian Emeishan large igneous province eruptions in SW China using conodont biostratigraphy and its bearing on mantle plume uplift models. Lithos. 2010;119(1):20–33. https://doi.org/10.1016/j.lithos.2010.05.012.

Tian YT, Feng QL, Li Q. The petrogenesis and sedimentary environment of the Bedded cherts from Upper Permian Dalong Formation, Southwest Guangxi. Acta Sedimentol Sin. 2007;25(5):671–7. https://doi.org/10.14027/j.cnki.cjxb.2007.05.003 **(in Chinese)**.

Taylor SR, McLennan SM. The continental crust: its composition and evolution. Malden: Blackwell; 1985. p. 1–328.

Tribovillard N, Algeo TJ, Lyons T, et al. Trace metals as paleoredox and paleoproductivity proxies: an update. Chem Geol. 2006;232(1):12–32. https://doi.org/10.1016/j.chemgeo.2006.02.012.

Van den Boorn SHJM, Van Bergen MJ, Vroon PZ, et al. Silicon isotope and trace element constraints on the origin of ~3.5 Ga cherts: implications for Early Archaean marine environments. Geochim Cosmochim Acta. 2010;74(3):1077–103. https://doi.org/10.1016/j.gca.2009.09.009.

Veevers JJ, Tewari RC. Permian–Carboniferous and Permian–Triassic magmatism in the rift zone bordering the Tethyan

margin of southern Pangea. Geology. 1995;23(5):467–70. https://doi.org/10.1130/0091-7613(1995)023%3c0467:PCAPTM%3e2.3.CO;2.

Wang RJ. Discovery of foraminifers in the Permian radiolarites in Jiangsu and Auhui Provinces and their depositional environment. J Tongji Univ. 1993;21(4):519–24 **(in Chinese)**.

Williams LA, Crerar DA. Silica diagenesis, II: general mechanisms. J Sediment Res. 1985;55(3):312–21. https://doi.org/10.1306/212F86B1-2B24-11D7-8648000102C1865D.

Wu SH, Feng ZZ, He YB. Study on anoxic environments of Permian in the middle and Lower Yangtze Region. Acta Sedimentol Sin. 1994;12:29–36. https://doi.org/10.14027/j.cnki.cjxb.1994.02.004 **(in Chinese)**.

Wu HR. Implications of radiolarian chert for the paleogeography of South China. J Paleogeogr. 1999;1(2):28–35 **(in Chinese)**.

Xu YT. Genetic geochemistry for the bedded silicalite in the late Permian Dalong formation and its sedimentary setting in southeastern Hubei. J Guilin Inst Technol. 1997;3:204–12 **(in Chinese)**.

Yamamoto K. Geochemical characteristics and depositional environments of cherts and associated rocks in the Franciscan and Shimanto terranes. Sediment Geol. 1987;52:65–108. https://doi.org/10.1016/0037-0738(87)90017-0.

Yao X, Zhou YQ, Li S, et al. Research status and advances in chert and Permian chert event. Adv Earth Sci. 2013;28(11):1189–200 **(in Chinese)**.

Yin HF, Song HJ. Mass extinction and Pangea integration during the Paleozoic–Mesozoic transition. Sci China Earth Sci. 2013;56:1791–803. https://doi.org/10.1007/s11430-013-4624-3.

Yin HF, Huang S, Zhang KX, et al. The effects of volcanism on the Permo–Triassic mass extinction in South China. In: Sweet WC, et al., editors. Permo–Triassic events in the Eastern Tethys. Cambridge: Cambridge University Press; 1992. p. 169–74.

Yin HF, Wu SB, Du YS, et al. South China defined as part of Tethyan archipelagic ocean system. Earth Sci J China Univ Geosci. 1999;21:1–12 **(in Chinese)**.

Yu H, Chen DZ, Wei HY, et al. Origin of bedded chert and organic matter accumulation in the Dalong Formation of Upper Permian in western Hubei Province. Acta Pet Sin. 2012;28(3):1017–27 **(in Chinese)**.

Zeng PS, Yang ZS, Meng YF, et al. Petrogenesis and significance of cherts in Tongling mineralization cluster area, Anhui. Geol Rev. 2004;50(2):153–61. https://doi.org/10.16509/j.georeview.2004.02.006 **(in Chinese)**.

Zhao ZG, Gao LM. Discussion about standardization of methods to calculate δEu and δCe. Report Stand. 1998;19(5):23–5 **(in Chinese)**.

Zhu HF, Qin DY, Liu CZ. The origin, distributive pattern and tectonic control of siliceous rocks in Gufeng and Dalong formations, South China. Exp Pet Geol. 1989;11(4):341–8 **(in Chinese)**.